

Local and segmental dynamics in homopolymer and triblock copolymers with one semicrystalline block

E. Laredo, M. C. Hernandez, and A. Bello

Physics Department, Universidad Simón Bolívar, Apartado 89000, Caracas, Venezuela

M. Grimau, A. J. Müller, and V. Balsamo

Materials Science Department, Universidad Simón Bolívar, Caracas, Venezuela

(Received 8 August 2001; published 23 January 2002)

Thermally stimulated depolarization currents, TSDC, experiments have been performed on a series of poly(styrene)-*b*-poly(butadiene)-*b*-poly(ϵ -caprolactone) triblock copolymers SBC with different proportions of the poly(ϵ -caprolactone) crystallizable block, PCL. The morphology of the segregated microphases varies with the PCL content and has been observed by transmission electron microscopy. The crystallinity of the PCL block is estimated by wide angle x-ray scattering, WAXS. The relaxation times distribution is extracted by a numerical decomposition of the TSDC spectra and it is shown that this distribution is not significantly changed on going from the homopolymer to the triblock copolymer with 16 wt % to 77 wt % of PCL in the original samples. Better segregation of the mesophase structure is reached when the samples are annealed at 413 K and important variations in the TSDC and WAXS spectra are observed as a result of the thermal treatment. For the $S_{09}B_{14}C_{77}$ triblock copolymer the results obtained can be explained by postulating the existence of a rigid amorphous phase in the PCL block. Such rigid amorphous phase is located between the core-shell cylinders formed by the other blocks [with poly(styrene)(PS) as core and poly(butadiene)(PB) as shell] and is constrained by undulated lamellae of crystalline PCL material. In the case of $S_{35}B_{15}C_{50}$ triblock copolymer, an important amount of diffuse PS-PCL interphase where the homopolymers are mixed must be present before annealing. The results for the material with the less abundant PCL block are explained as a result of the confinement in nanotubes of PCL surrounded by PB embedded in a vitreous PS matrix. Broadband dielectric experiments on these same materials confirm the results obtained by TSDC spectroscopy.

DOI: 10.1103/PhysRevE.65.021807

PACS number(s): 36.20.-r, 77.22.Gm, 77.84.Jd, 64.70.Pf

I. INTRODUCTION

Biodegradable and nontoxic polymers can be used in the controlled release of pharmaceutical drugs from implanted devices. Poly(ϵ -caprolactone) (PCL) applications in this field are somewhat limited due to the lifespan of the device, approximately one year, and to its semicrystalline character with high crystallinity degree. Blending this homopolymer or using it as a component in block copolymers has been considered as an alternative in order to reduce the biodegradation rate and to improve its mechanical properties by controlling its crystallinity. More generally, there are applications of block copolymers in the industry of adhesives, surfactants, and compatibilizers in polymer blends. The association of immiscible components as block copolymers offers a broad and interesting field because of their characteristic properties due to the formation of highly organized structures into mesophases, the morphology of which has been deeply studied by transmission electron microscopy, x-ray and neutron scattering when the material is in the ordered state. The order-disorder transition observed as the temperature increases or the molecular weight diminishes is determined by the product $\chi \times N$ for each composition, χ being the Flory-Huggins segment-segment interaction parameter and N the polymerization degree. In the ordered state the microphase segregation is characterized by long range order in the composition, and by characteristic sizes in the order of tens of nanometer. The existence of the various morphologies reported for these materials is the result of a competition among enthalpic and

entropic contributions to the free energy [1].

In recent years a great number of works have been devoted to the study of the resulting morphology and its influence on the dielectric and mechanical properties of the diblock [1–5] and triblock [6–8] copolymers. Most of these studies are performed on block copolymers made from amorphous blocks such as poly(styrene)-*b*-poly(isoprene), poly(isoprene)-*b*-poly(butadiene), and poly(ethylenepropylene)-*b*-poly(ethylene). Most of them can be considered as thermoplastic elastomers due to the union of a rubbery block to a rigid one in its glassy state. The introduction of one semicrystalline block has been achieved and diblock copolymers poly(oxyethylene)-*b*-poly(oxybutylene) [9] have been studied by dielectric spectroscopy, poly(ϵ -caprolactone)-*b*-poly(butadiene) [10,11] and poly(ϵ -caprolactone)-*b*-poly(styrene) [12] by calorimetry and x-ray scattering. Also, the triblock copolymer poly(styrene)-*b*-poly(butadiene)-*b*-poly(ϵ -caprolactone) PS-*b*-PB-*b*-PCL and the hydrogenated poly(styrene)-*b*-poly(butadiene)-*b*-poly(ϵ -caprolactone), PS-*b*-PE-*b*-PCL, with one and two crystallizable blocks have been synthesized and thermally characterized [13,14]. The observed morphology is in this case determined by the combined effect of the energy reduction resulting from the microphase separation and the crystal formation within the crystallizable block. In the case of high molecular weight polymers in the strong segregation state, the microphase structure established at high temperatures cannot be destroyed by the crystallization process that takes

place at lower temperatures and the lamellae are formed with boundary conditions imposed by the mesophases structure. Additionally, the amorphous block has a glass transition temperature T_g higher than the crystallization temperature of the crystallizable block T_c thus introducing a further restriction to the chain mobility that will have an effect on the subsequent crystallization. On the other side, if the crystallizable block is bonded to a polymer that at T_c is in the molten state, the crystallization that occurs within the microdomain structure should be similar to that of the homopolymer due to the softness of the neighboring block. Nojima and coworkers [10,12] have studied the crystallization of poly (ϵ -caprolactone) in diblock copolymers, PB-*b*-PCL and PS-*b*-PCL, where the crystallization temperature of the PCL block is ca. 323 K in between the glass transition temperature of PS, $T_{gPS}=368$ K, and that of the PB, $T_{gPB}<T_{cPCL}$. In the case of the diblock PB-*b*-PCL the microdomain structure is fixed by chemically cross linking the PB blocks and the PCL blocks crystallize in the same crystal form as in the homopolymer; the microdomain structure in the melt remains practically unchanged after the crystallization process. In the diblock with an untreated PB block the microdomain structure is completely replaced by a lamellar morphology upon crystallization. In PS-*b*-PCL the crystallization behavior is studied as a function of T_{gPS} that is varied by adding controlled amount of a plasticizer miscible only with the PS block and it was demonstrated that the PCL block is only partially crystallized when T_{gPS} was lower than T_{cPCL} . When the crystallization takes place the morphology detected by the long spacing and lamellar thickness estimates, is not affected by the presence of the plasticized PS block. When the molecular weight of the PS chain is varied Heuschen, Jerome, and Teyssié [11] have shown with electron, optical microscopy, and differential scanning calorimetry (DSC) that there is a strong variation for the polymer miscibility. As the length of the PS increases one goes from the existence of a large diffuse interphase that involves most of the volume of the material to a sharp phase separation.

The study of the dielectric relaxations in these multiphase materials needs the presence of molecular segments with a dipolar moment. PCL that belongs to the A2-type polymers is dielectrically active due to the presence of a dipolar moment perpendicular to the main chain in addition to a monomeric dipole parallel to the backbone. The end-to-end vector being configuration dependent, its variation shows in the dielectric spectrum as a normal mode observed at low frequencies and high temperatures. Dielectric spectroscopy experiments performed at room temperature on semidilute [15] and dilute solutions [16,17] of PCL have evidenced the presence of this normal mode. A previous broadband dielectric study (BBDS) [18] on the PCL homopolymer has shown a very rich and complicated dielectric spectrum composed of low temperature γ and β modes due to localized molecular motions and the segmental primary relaxation originated by cooperative rearrangements near the glass transition temperature. At higher temperatures a complicated peak appears, labeled α' , which is superposed to the dc conductivity contribution and which has been attributed to a Maxwell-Wagner-Sillars (MWS) interfacial polarization release after

detailed thermally stimulated depolarization currents (TSDC) studies [19], in agreement with the assignment by Vanderschueren, Ladang, and Heuschen [20]. In this latter work TSDC techniques are used to study, besides the homopolymer, diblock copolymers PS-*b*-PCL with a styrene wt% ranging from 30–74%. The temperature of the maximum of the primary or α relaxation remains constant for PCL contents higher than 50% in weight that indicates the existence of two segregated phases. Only the 74 wt% copolymer that is totally amorphous shows a shift of $T_{m\alpha}$ towards lower temperatures, which cannot then be attributed to molecular mixing of the two blocks but is rather ascribed to the absence of the restrictions imposed in the other compositions by the presence of a crystalline phase. The high temperature peak is attributed to the free charge carriers piled up at polymer interfaces, its position and intensity being related to a diminution of the ionic mobility due to the increase of PS content. It has also been demonstrated in PS-*b*-PI-*b*-PS [7] that the conformational motions of the poly(isoprene) (PI) blocks, as detected by BBDS, are seriously affected by preannealing at $T>T_{gPS}$.

The present paper reports the dielectric studies, i.e., TSDC and BBDS, on triblock copolymers based on the semicrystalline poly(ϵ -caprolactone) with molten PB blocks bonded to rigid PS blocks on the other side. These materials in the segregated state present a rich variety of morphologies [21,22] depending on the weight proportion of the constituents, where the lamellar structure usually found for the PS-*b*-PCL, includes small PB cylinders located at the PS-PCL interfaces for $S_{35}B_{15}C_{50}$ copolymer. For the richest and weaker PCL content the microdomains are concentric cylinders embedded in the predominant phase, the less abundant being in the center of the microdomain. Then, by sweeping the composition range for PCL in PS-*b*-PB-*b*-PCL the effect on the molecular motions probed dielectrically of the confinement in mesophases of known shape and dimensions, can be studied. Additionally, the existence of a variety of interfaces besides the amorphous-crystalline regions of PCL might cause changes in the interfacial polarization peaks that occur in the homopolymer. The extension of these intermediate regions as a result of the thermal treatment of the samples in order to optimize the segregation process, is also the object of this work and it will be shown that the final morphology has a very strong effect on the amount of amorphous phase and on its mobility.

II. EXPERIMENTAL SECTION

A. Materials

The PCL homopolymers were from two different origins. The samples with average molecular weights determined by gel permeation chromatography, $\bar{M}_n=17\,000$, $57\,000$, $100\,000$ g/mol and a polydispersity lower than 1.6 were from Aldrich Chem. Co. Inc. The PCL used for the synthesis of the copolymers, PCL⁹³, was prepared by successive anionic polymerization in benzene with an average molecular weight $\bar{M}_n=93\,000$ g/mol and a polydispersity of 1.4. The block copolymers used in the present work were prepared by sequential anionic polymerization of styrene, butadiene, and

TABLE I. Molecular characteristics of the homopolymer, poly(ϵ -caprolactone), PCL, and the triblock copolymers poly(styrene)-*b*-poly(butadiene)-*b*-poly(ϵ -caprolactone) SBC.

Sample ^a composition	$\bar{M}_{n,\text{copolymer}}^b$ (10^{-3} g/mol)	$\bar{M}_{n,\text{PCL}}^b$ (10^{-3} g/mol)	PB microstructure		\bar{M}_w/\bar{M}_n^c
			1,4 units (%)	1,2 units (%)	
PCL		93			1.4
S ₀₉ B ₁₄ C ₇₇	181	140	59	41	1.47
S ₃₅ B ₁₅ C ₅₀	150	75	89	11	1.22
S ₅₇ B ₂₇ C ₁₆	137	22	88	12	1.12

^aThe subscripts indicate the weight percent of each block.

^bCalculated from ¹H NMR.

^cSEC, calibrated with polystyrene standards.

ϵ -caprolactone (ϵ -CL) in benzene. Sec-Butyl lithium was used as initiator and 1,1 diphenyl-ethylene as capping agent for the crossover reaction from polybutadienyl lithium to ϵ -caprolactone. The polymerization time of the ϵ -CL was limited to about 4 min to avoid side reactions. The details of the synthesis are described elsewhere [13]. The molecular characteristics of the materials, shown in Table I, were determined through size exclusion chromatography (SEC) calibrated with PS-standards and ¹H-nuclear magnetic resonance spectroscopy. The samples for TSDC and BBDS measurements were prepared using two methods: (a) Films of about 200 μm thick were prepared by compression molding at 453 K for S₅₇B₂₇C₁₆ and 423 K for the other copolymers. After a molding time of 3 min the films were quenched in air at 298 K. These samples will be referred as in the original state. (b) The films prepared in (a) were subsequently annealed at 413 K for 3 h under nitrogen atmosphere and slowly cooled (at approximately 1 K/min) to 318 K and kept at that temperature for another 3 h. Finally they were cooled down to room temperature. The films with this treatment will be referred as the annealed samples. It should be mentioned that when the samples were compression molded at 423 K or 453 K for 3 min they were in a microphase separated molten state. These poly(styrene)-*b*-poly(butadiene)-*b*-poly(ϵ -caprolactone), SBC block copolymers remain microphase separated even at temperatures as high as 523 K, where degradation of the copolymers begins [23]. Annealing at 413 K for a long period of time will only accentuate phase separation causing better definition of the microphase separated morphologies and it is a procedure

commonly used as part of the sample preparation technique for observation in the transmission electron microscope [24]. A Perkin-Elmer DSC-7 with an ultrapure nitrogen atmosphere has been used, the calibration was performed with indium and tin standards. From the compression molded films small disc samples (with diameters much larger than their heights) were cut, so that their weight, in all cases, was approximately 10 mg. Table II shows the thermal characteristics of the samples obtained from DSC measurements. The samples prepared according to the procedure (a) described above were first cooled in the DSC from 298 K (the loading temperature) down to 248 K at a rate of 40 K/min, then a heating scan was performed from 248 K to 393 K at 10 K/min. Table II shows that the three copolymers employed exhibit the characteristic transitions corresponding to their constituent blocks at positions that are generally independent of the block copolymer composition. The onset melting temperature (T_{mo}) of the PCL block is very similar to that of neat PCL. The block copolymer S₅₇B₂₇C₁₆ exhibits a fractionated crystallization phenomenon in view of its small PCL content [13,25,26], so its crystallization occurs in at least two steps, one of which is above 248 K but the other is closer to the PCL T_g at temperatures around 213 K. This is the reason why this sample has a much lower degree of crystallinity as compared to the other two copolymers [14,25,26], since it was only cooled down to 248 K and it has not finished its crystallization process.

B. Thermally stimulated depolarization currents

The experimental setup used to perform the TSDC characterization has been designed in our laboratory [27]. The

TABLE II. Thermodynamics characteristics of the homopolymer, poly(ϵ -caprolactone) PCL and the triblock copolymers poly(styrene)-*b*-poly(butadiene)-*b*-poly(ϵ -caprolactone) SBC.

Sample	$T_g(\text{PB})^a$ (K)	$T_g(\text{PCL})^a$ (K)	$T_g(\text{PS})^a$ (K)	T_{mo} (K)
PCL ⁹³		207		325
S ₀₉ B ₁₄ C ₇₇	193	208		325
S ₃₅ B ₁₅ C ₅₀	174	208	378	323
S ₅₇ B ₂₇ C ₁₆	178	206	378	325

^aData from Ref. [14].

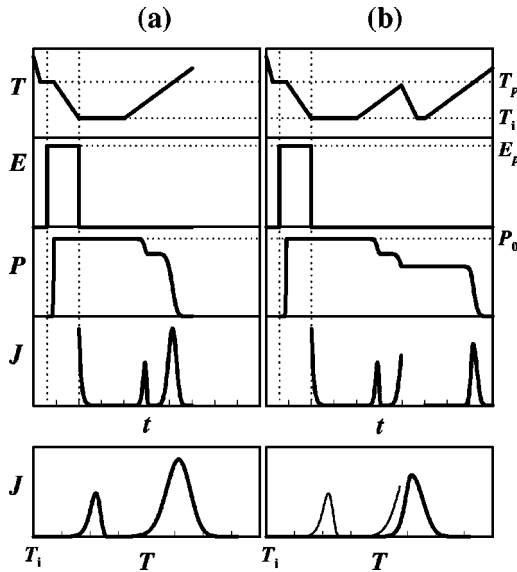


FIG. 1. Experimental protocol for the TSDC measurements with the variation of the temperature T , the applied field E , the polarization acquired by the sample P , and the depolarization current density J_D . (a) standard polarization procedure (b) peak cleaning procedure.

polarization step is performed at constant temperature in a nitrogen atmosphere, the cell being previously thoroughly evacuated to avoid humidity traces. During the depolarization stage the sample is heated at a constant rate of 0.07 K/s in a helium atmosphere at a pressure of 150 Torr from 77 K to above the polarization temperature T_p . The temperature control system allows to regulate the depolarization process at a constant heating rate that induces the TSDC current measured with a Keithley 642 electrometer connected in series to the measuring cell where the sample is located between two metallic electrodes. The samples are disk shaped compression molded films, 20 mm in diameter and with an average thickness of 300 μm .

The TSDC characterizations can be differentiated by two types of polarization protocols whose sequences are shown in Fig. 1. In the first polarization protocol, Fig. 1(a), the electric field is applied during a time t_p (typically 3 min) at a polarization temperature T_p , and during the cooling of the sample to 77 K; the global TSDC peak is recorded as the temperature increases at a linear rate. A “clean peak” is obtained when the sample is discharged by heating to a temperature from 10 to 30 K below the maximum of the peak T_m as shown in Fig. 1(b). Then the sample is quenched again to low temperatures before recording the “clean” TSDC spectrum as the temperature is raised at a constant rate. This particular protocol allows the isolation of the α relaxation from the secondary processes thermally activated at lower temperatures.

The first polarization protocol is used here to generate the spectra studied by the direct signal analysis, DSA, numerical decomposition. The clean curves for the α relaxation obtained with the second polarization program are analyzed with the simulated annealing direct signal analysis, SADSA computer procedure [28]. These numerical decompositions

in elementary Debye processes allow the extraction of the relaxation time distribution for each sample and enable the comparison of the molecular dynamics that occur in the different temperature regions originated by local or segmental motions.

C. Broadband dielectric spectroscopy

Frequency domain measurements of the real and imaginary part of the dielectric function were performed at $1 \times 10^{-2} \text{ Hz} \leq \nu \leq 3 \times 10^6 \text{ Hz}$ with a Concept Twelve system (Novocontrol GmbH, Hundsangen, Germany) integrating an impedance /gain phase analyzer (Solartron SI 1260) and a broadband dielectric converter. Isothermal measurements were performed on compression molded films, 30 mm in diameter and about 0.3 mm thick, slowly cooled to room temperature. The molding was performed at 393 K. Gold electrodes were carefully sputtered on the PCL samples used for the low and high frequency experiments. The temperature control is very efficient yielding a thermal stability better than 0.1 K for each temperature step. The isothermal experiments were performed from 133 to 313 K each 2 K, that is below the melting temperature of the crystalline regions in PCL.

D. Transmission electron microscopy

The samples for transmission electron microscopy (TEM) were prepared following a procedure that can ensure good definition of the microphase separated morphology. Films of 0.5–1 mm in thickness were cast from a dilute toluene solution. After drying, the films were annealed at 413 K under nitrogen atmosphere for 2 h and then cooled down to 315 K, where the sample was left to crystallize for 5 h before quenching to room temperature. Ultrathin sections were cryogenically cut using a FC4 Reichert Ultramicrotome and the sections were stained by Osmium Tetroxide. The observations were performed with a Philips electron microscope at 80 kV.

E. Wide angle x-ray scattering

The crystallinity degree X_c of the homopolymer and block copolymers was determined by conventional wide angle x-ray scattering (WAXS) with Ni-filtered Cu $K\alpha$ radiation. The unit cell of PCL is orthorhombic and it crystallizes in the noncentrosymmetric space group $P2_12_12_1$ with cell constants [29,30] $a=7.496 \text{ \AA}$, $b=4.974 \text{ \AA}$, $c=17.297 \text{ \AA}$. The X_c value is estimated by analyzing the WAXS spectrum after background corrections, from $5^\circ \leq 2\theta \leq 34^\circ$ in terms of Gaussian peaks, the widest ones being the contributions of the amorphous regions. A value for the crystallinity of the homopolymer $X_c=53\%$ is found that is comparable to the DSC result on the same material (47%). In the case of the triblock copolymers the determination of X_c is more difficult as the double-featured peak scattered from amorphous PS and PB blocks occurs in the same angular region as the scattering by the amorphous and crystalline regions of the PCL blocks. However, the variation of the crystallinity with the

annealing described above in order to reach an optimum segregated microdomain structure has been estimated.

III. RESULTS AND DISCUSSION

A. Morphology studies

In these semicrystalline block copolymers the microphases segregated at high temperature are affected by the joint influence of the crystallization and microphase separation. The resulting morphology must influence the observed dielectric relaxations as the confinement in nanostructures and the neighborhood with rigid or melted chains will result in variations of the chain mobility that can be detected by analyzing the relaxation time distribution for each block copolymer and comparing it with the homopolymer. The PCL homopolymer is a semicrystalline polymer that develops spherulites upon dynamic as well as isothermal crystallization. It has been demonstrated that the spherulitic superstructure persists in SBC block copolymers when the PCL block conforms the matrix. *ABC* triblock copolymers can develop fascinating morphologies because the microphase separation is determined by the balance of three interaction parameters χ_{AB} , χ_{AC} , and χ_{BC} and two composition variables [24].

Figure 2(a) shows a TEM micrograph corresponding to $S_{57}B_{27}C_{16}$ triblock copolymer. Due to the staining conditions employed, PB should appear as the darkest component, PS should be gray, and PCL will not be stained and will therefore appear white. The three phases are very clear from the TEM picture, the PS forms the matrix as one would expect in view of its predominant content in the copolymer. The PB forms the edge-shaped black shell surrounding the PCL bright cores. The bottom part of the micrograph shows a lateral view of the PCL rods or cylinders that conform the bright cores, while the top part shows the cross section. A schematic diagram of the morphology can be seen in the top right hand corner of the micrograph. A previous detailed morphological study of this copolymer [22] demonstrated that the crystallization of the PCL block does not change significantly the basic morphology, but it affects the shape of the microdomains since the $S_{57}B_{27}C_{16}$ triblock copolymer exhibits a polygonal core-shell morphology in a PS matrix. This morphology is probably the result of crystallization within the originally cylindrical cores that were deformed in order to accommodate PCL crystallites [22].

As the amount of PCL is increased in the block copolymers, the morphology changes as expected. Figure 2(b) shows how the $S_{35}B_{15}C_{50}$ block copolymer exhibits a lamellar morphology where stacks of PS and PCL lamellae alternate with PB cylinders located at the lamellar interphase. This morphology is very similar to that exhibited by the copolymer with composition $S_{27}B_{15}C_{58}$ and it has been described in detail previously [21]. Finally, Figure 2(c) shows a TEM micrograph of the $S_9B_{14}C_{77}$ block copolymer. It is clear that the matrix is now the PCL (as expected from its 77% composition) and within it, cylinders of PS are surrounded by a shell of PB, i.e., a core-shell cylinder-type morphology. The morphology is schematically shown in the top right hand corner and is based on extensive observations previously reported for this block copolymer [31]. One peculiar

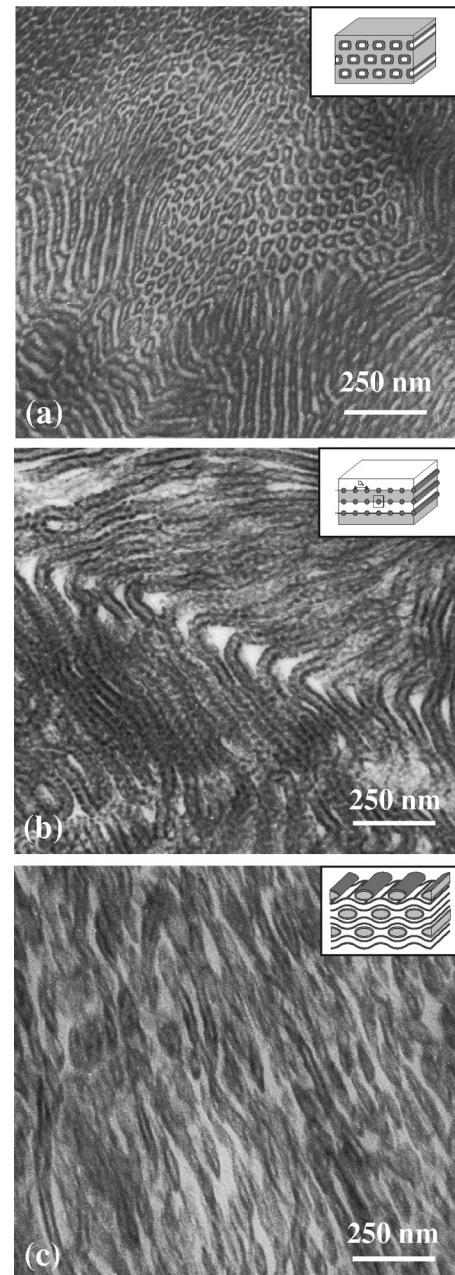


FIG. 2. TEM micrographies of the different triblock copolymer morphologies studied: (a) $S_{57}B_{27}C_{16}$, (b) $S_{35}B_{15}C_{50}$, (c) $S_{09}B_{14}C_{77}$. On the upper right corner is a schematic drawing of the microstructures observed.

aspect of this morphology is the ellipsoidal cross section of the core-shell cylindrical morphology. Such deformation of the amorphous microphases has been attributed to the topological influence of the PCL crystallizing chains in the surroundings of the core-shell structure. It should also be mentioned that this copolymer forms spherulites during isothermal crystallization at temperatures well below the T_g of the PS block, since this may be connected to the deformation experienced by the amorphous microdomains, although this fact is still not clear [31].

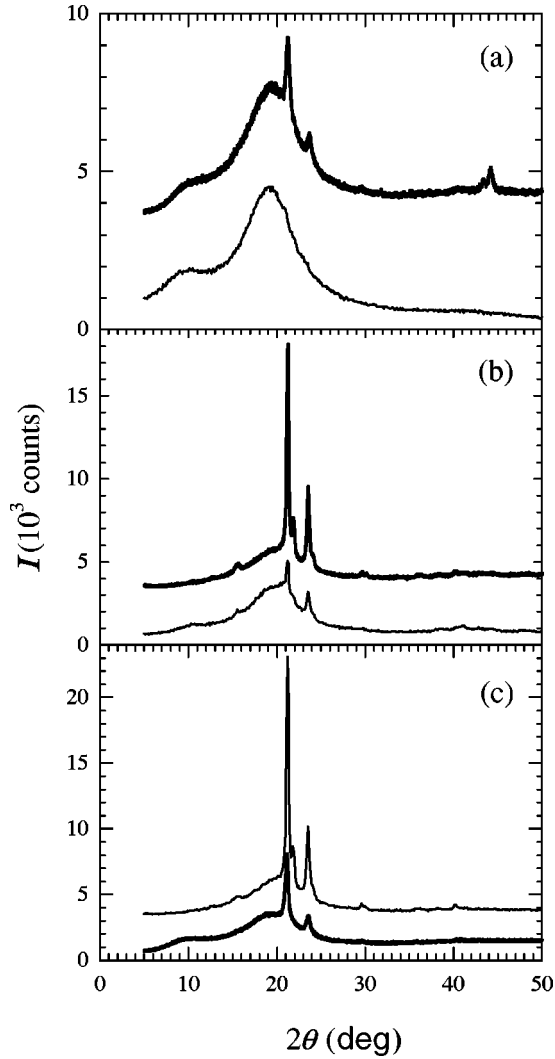


FIG. 3. WAXS spectra for the three block copolymers studied, in original conditions (thin line) and after annealing (thick line): (a) $S_{57}B_{27}C_{16}$, (b) $S_{35}B_{15}C_{50}$, (c) $S_{09}B_{14}C_{77}$.

B. Crystallinity results

As the dipoles that contribute to the polarization of the sample for each relaxation mode are located in the amorphous zone, it is important to estimate the crystallinity degree for the PCL block and whether it changes when the annealing to favor the segregation is performed. The WAXS traces from $5^\circ \leq 2\theta \leq 50^\circ$ for the three triblock copolymers in the original and annealed states are represented in Figs. 3(a–c) for increasing PCL contents. The values of the crys-

tallinity degree X_c are reported in Table III for the PCL homopolymers with different molecular weights and for the triblock copolymers in the original and annealed state. It is observed that the block copolymer with the richest PCL content in the original state [Fig. 3(c) thin line] shows a high crystallinity that has been estimated to be 53% by WAXS. However, when the annealing is performed the PCL crystal reflections decrease steeply as shown in this same figure with a thick line and X_c is now estimated to be 23%. The next triblock copolymers with less PCL, $S_{35}B_{15}C_{50}$ and $S_{57}B_{27}C_{16}$, show the opposite variation, i.e., the PCL degree of crystallinity increases from 23% to 54% and from 4% to 18%, respectively, as the annealing at 413 K is performed and the mesophases are best segregated. These crystallinity variations, will prove to be very useful for the better understanding of the variations observed in the dielectric spectrum after annealing.

C. TSDC experiments

The current caused by the disorientation of the dipolar entities in a TSDC experiment is written for a single Debye process as

$$J_D(T) = \frac{P_0}{\tau(T)} \exp\left(-\frac{1}{b} \int_{T_i}^T \frac{dT'}{\tau(T')}\right), \quad (1)$$

where b is the linear heating rate, $\tau(T)$ is the relaxation time of the dipolar species under consideration, P_0 is the built-in polarization at the effective polarization temperature T_p and is a function of the number of dipolar orientable segments N_d in the polarizing field E_p and of their effective dipolar moment μ given by

$$P_0 = \frac{N_d \mu^2 E_p}{3kT_p}. \quad (2)$$

The temperature dependence of the relaxation times involved is described by an Arrhenius equation for the local low temperature modes, with an activation energy E_a and a preexponential factor τ_0

$$\tau(T) = \tau_0 \exp\left(\frac{E_a}{kT}\right) \quad (3)$$

and for the segmental mode by a Vogel-Tammann-Fulcher (VTF) expression

TABLE III. WAXS crystallinity determinations for the homopolymers, poly(ϵ -caprolactone) PCL and the triblock copolymers poly(styrene)-*b*-poly(butadiene)-*b*-poly(ϵ -caprolactone) SBC (X_c in %)

PCL $M_n/1000$	PCL ¹⁷	PCL ⁵⁷	PCL ⁹³	PCL ¹⁰⁰
	79	64	65	64
Copolymers		$S_{09}B_{14}C_{77}$	$S_{35}B_{15}C_{50}$	$S_{67}B_{27}C_{16}$
	Original	53	23	4
	Annealed	23	54	18

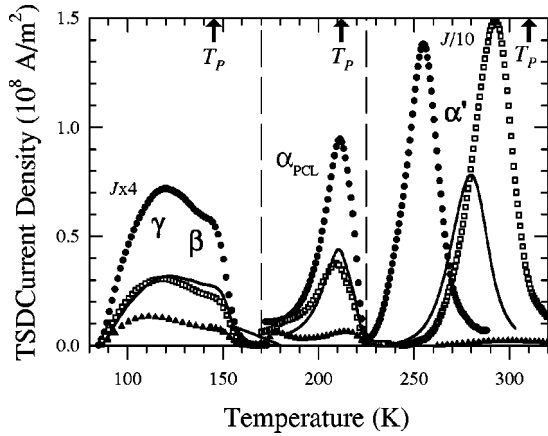


FIG. 4. TSDC spectra for the block copolymers and the PCL homopolymer: (●) PCL, (△) $S_{57}B_{27}C_{16}$, (□) $S_{35}B_{15}C_{50}$, (line) $S_{09}B_{14}C_{77}$. The polarization temperatures are indicated by arrows.

$$\tau_{VTF}(T) = \tau_0' \exp\left(\frac{E_{VTF}}{k(T-T_0)}\right) = A \exp\left(\frac{B}{(T-T_0)}\right), \quad (4)$$

where T_0 is the temperature where the molecular motions are frozen. In complex materials with complicated energy landscape, as seen by the reorienting dipolar segments, the description of the recorded TSDC peaks needs the assumption of the existence of a two-dimensional (2D) distribution (both in E_a and τ_0) of relaxation time. This can be performed experimentally by using narrow polarization windows and analyzing the small peaks obtained by this thermal sampling technique as Debye peaks, or by decomposing the global TSDC peak numerically. The DSA and the SADSAs have been described in detail previously [27,28]. The advantage of the numerical decomposition is the absence of assumptions on the profile of the distribution and the use of true Debye peaks that contribute P_{0i} to the total polarization that can be determined by the area under the TSDC curve that is equal to bP_0 A K/m². The sums of squared residuals χ^2 are as low as 10^{-9} after the fitting of the experimental peak whose P_0 has been normalized to 1. The TSDC spectra $J(T)$ obtained with the PCL and the triblock copolymers in the original state can be divided into three regions that are represented in Fig. 4. The polarization temperatures for each zone have been chosen in order to minimize the effect of higher temperature peaks and are indicated in the figure. All the curves in this figure have been normalized to a field of 100 MV/m.

1. Homopolymer and original triblock samples

The lowest temperature zone, $T \leq 170$ K, shows the presence of a multicomponent weak peak with two main broad relaxations that have been labeled γ and β . The numerical decomposition of this broad peak into elementary modes leads to the determination of the 2D (E_i and τ_{0i}) Arrhenius relaxation time distribution that is shown in Fig. 5 for the PCL⁹³ homopolymer. The fitting of the experimental curve [Fig. 5(a)] is excellent with a sum of squared residuals in the range of $\chi^2 \approx 10^{-9}$ for a normalized area corresponding to a unit polarization. The energy histogram plotted in Fig. 5(b)

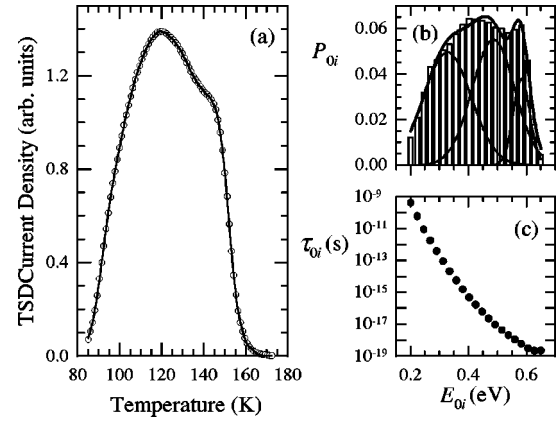


FIG. 5. Results of the DSA for the secondary relaxations in the homopolymer poly(ϵ -caprolactone): (a) experimental data and fitted profile; (b) energy histogram showing the contribution to the total polarization of each Debye process; (c) variation of the preexponential factor with the energy bin value for the Debye processes whose sum best describe the experimental profile.

shows the contribution to the total polarization P_{0i} of each Debye peak with energy E_i and preexponential factor τ_{0i} ; the variation of τ_{0i} with E_i is represented in Fig. 5(c). The histogram can be decomposed in three main relaxations with Gaussian profiles that are drawn in Fig. 5(b). These relaxations have been studied [18] as a function of the crystallinity for PCL with different molecular weights ($17\,000 \leq \bar{M}_n \leq 100\,000$) the resulting crystallinity degrees being 79% for $\bar{M}_n = 17\,000$ g/mol and 64% for $\bar{M}_n \geq 57\,000$ g/mol, without finding any significant differences either in the position of the current density maxima, $T_{m\gamma}$, $T_{m\beta}$, or in the relaxation time distribution which shape and position of the maxima do not change.

In Table IV the results from the analysis for the PCL homopolymer are given in the first row. The only variations observed for the homopolymers is on the areas under the $J(T)$ curve ($85 \text{ K} \leq T \leq 170 \text{ K}$) that is representative of the number of dipoles whose orientation contributes to the total polarization. The area under the $J(T)$ curve, $bP_{0\gamma\beta}$, for the different crystallinity degrees obtained as the molecular weight increases, varies linearly with $(1 - X_c)$. For the homopolymers it is also found that there exists a linear relationship between the area under the α peak and that of the low temperature peak ($\gamma + \beta$). This is equivalent to say that the amorphous zones detected by measuring X_c by WAXS in the homopolymers are also contributing to the polarization frozen in a TSDC experiment. As the molecular motions responsible for the γ and β modes are localized and less affected by the morphology of the sample, the $bP_{0\gamma\beta}$ values are assumed to be representative of the amount of the amorphous regions in the homopolymers.

In Fig. 4 the TSDC low temperature traces corresponding to the PCL block in the original copolymers are also represented. The DSA numerical decomposition performed on the triblock copolymers shows that there is no significant change in the profile of the distribution except for the $S_{57}B_{27}C_{16}$ where the γ_1 and γ_2 peaks are slightly shifted to lower temperatures and consequently to lower reorientation energies,

TABLE IV. Relaxation parameters of the homopolymer, poly(ϵ -caprolactone) PCL and the triblock copolymers poly(styrene)-*b*-poly(butadiene)-*b*-poly(ϵ -caprolactone) SBC.

Sample	γ_1		γ_2		β		α		m	
	T_m (K)	E_m (eV)	T_m (K)	E_m (eV)	T_m (K)	E_m (eV)	T_m (K)	E_m (eV)		
PCL ⁹³	109±2	0.327	131±2	0.486	148±2	0.583	211.3±0.5	0.15	55	
Original										
S ₀₉ B ₁₄ C ₇₇	106±2	0.298	129±2	0.449	148±2	0.572	210.5±0.5	0.15	57	
S ₃₅ B ₁₅ C ₅₀	107±2	0.318	131±2	0.475	147±2	0.585	210.3±0.5	0.15	57	
S ₅₇ B ₂₇ C ₁₆	101±2	0.286	121±2	0.409	147±2	0.569	214.6±0.5	0.17	56	
Annealed										
S ₀₉ B ₁₄ C ₇₇	105±2	0.300	128±2	0.454	148±2	0.569	210.0±0.5	0.14	54	
S ₃₅ B ₁₅ C ₅₀	107±2	0.326	133±2	0.489	148±2	0.590	210.1±0.5	0.15	57	
S ₅₇ B ₂₇ C ₁₆	103±2	0.287	125±2	0.430	150±2	0.569	221.2±0.5	0.20	55	

as seen in Table IV from rows 2 to 4. However, even in the material with the highest amorphous content, the intensity ratio of the β to γ peak remains unaltered and our experiments do not confirm the interpretation proposed in a previous study [20] where the equivalent of our β peak was attributed to a crankshaft motion originated within the crystalline phase. Within the experimental error one can see that the kinetic parameters of the low temperature modes that correspond to very localized molecular motions are not noticeably affected in the PCL richest triblock copolymer. The changes observed in the most confined and less abundant PCL triblock copolymer are the only significant effect of the existence of mesophases present in the original materials. However, the intensities of the peaks in the γ - β region are strongly affected if they are compared with what they should be if all the amorphous phase amount detected by WAXS was contributing to the intensity of these low temperature peaks. In other words, the amount of amorphous mobile phase determined by TSDC intensity in the γ - β region does not follow the same behavior as the homopolymers as a function of $(1 - X_c)$, when the measured intensity has been corrected for the abundance of PCL present in the copolymer. The three original triblock copolymers show less intense peaks evidencing the presence of an important quantity of amorphous phase that is not contributing to the TSDC peaks, i.e., dipoles that are not reorienting but which do not belong to crystalline regions of the PCL block within the triblock copolymer. The most important effect is shown in S₅₇B₂₇C₁₆ that has only 4% of crystallinity and which even when normalized to a 100% abundance is far below the trend defined by the homopolymers.

The next temperature zone in Fig. 4 ($170 \text{ K} \leq T \leq 225 \text{ K}$) shows the presence of the α peak of PCL at 211 K that corresponds to the cooperative motion of the dipolar molecular segments and it is the dielectric manifestation of the glass transition of PCL. For the two richest samples in polybutadiene component a small peak at 180 K is visible and it is attributed to the glass transition of PB. The polarization corresponding to the correlated reorientation of the mobile dipolar segments, i.e., the amount of mobile amorphous phase at the scale of these cooperative motions, is

represented by the area under the α curve shown in Fig. 4 for the original samples. The copolymer with the less abundant PCL phase is the only one that shows a slight shift of T_g to higher temperatures (+3 K as compared to PCL⁹³).

The analysis of the α peak is performed by decomposing the clean peak in elementary Debye processes with VTF relaxation times. The numerical decomposition is performed with the SADS procedure on clean curves in order to minimize the contribution of the components at $T \leq T_g$ that are still best described by Arrhenius relaxation times. The experimental protocol applied is described in Fig. 1(b). The VTF energies of the most intense elementary peak are given in Table IV together with the position of the α peak in the global spectrum. The VTF temperature is $T_0 = 157.5 \text{ K}$ for the best fit reached. A typical output of the SADS program is shown in Fig. 6 for the fitting of the α relaxation of S₀₉B₁₄C₇₇ in the original state. The knowledge of the VTF energies allows to calculate the fragility index m of the copolymers with the T_g and E_m values given in Table IV; the last column represents the m values for the materials studied

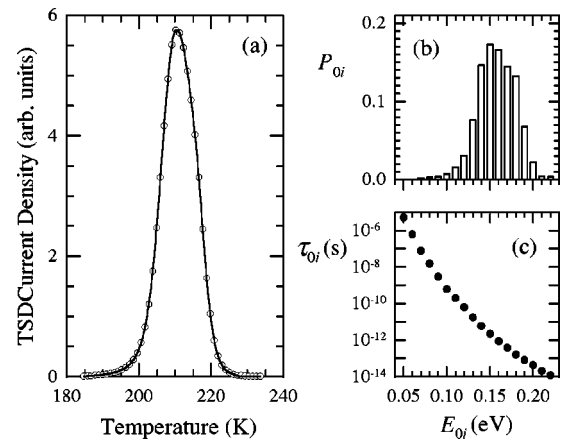


FIG. 6. Results of the SADS for the α relaxation in the block copolymer S₀₉B₁₄C₇₇: (a) experimental data and fitted profile; (b) energy histogram showing the contribution to the total polarization of each Debye process; (c) variation of the preexponential factor with the energy bin value, $T_0 = 157.5 \text{ K}$.

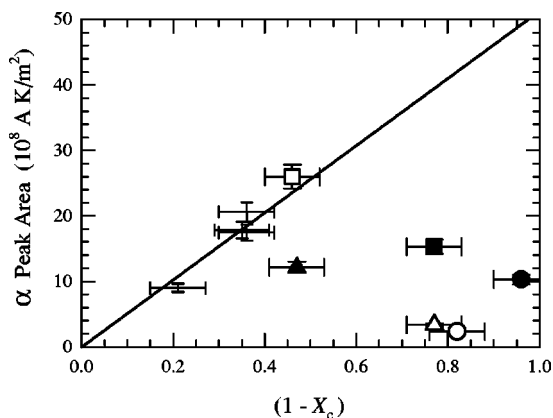


FIG. 7. Comparison of the amount of amorphous phase detected dielectrically, and the amorphous phase detected by WAXS, α peak area vs $(1 - X_c)$, for all the block copolymers and the PCL homopolymers. The filled symbols represent the original and the empty ones the annealed copolymers. + PCL homopolymers, (\circ) $S_{57}B_{27}C_{16}$, (\square) $S_{35}B_{15}C_{50}$, (\triangle) $S_{09}B_{14}C_{77}$.

here. It is found that the fragility indexes in the original materials are almost equal within 1% error. In conclusion the original triblock copolymers present similar kinetic parameters on going from the homopolymer to the less PCL rich triblock copolymer. However, when the area under the α peak is plotted vs $(1 - X_c)$ as shown in Fig. 7, the original samples represented by filled symbols, evidence a significant difference with the relationship found in the homopolymers. The continuous line in Fig. 7 represents the linear dependence fitted for the homopolymers with different molecular weights as a function of their amorphous content

$$bP_{0\alpha} = 51(1 - X_c).$$

If the amorphous phase measured by TSDC, that is the mobile one, is the same as that detected in the crystallinity determinations by WAXS as is the case in the homopolymers (+ in Fig. 7) the intensity measurements would fall on the solid line drawn in this figure when the amount of PCL is normalized to 100%. This is obviously not the case and on going from $S_{09}B_{14}C_{77}$ to $S_{57}B_{27}C_{16}$ the quantity of undetected amorphous phase increases as a result of the morphology, the existence of interphases, and the crystallization of PCL segregated in the lamellar or tubular morphologies described above. To clarify this effect the triblock samples were thermally treated in order to optimize the phase segregation and to study the changes that this better microphase separation would induce in the TSDC spectrum sensitive to the mobile amorphous phase alone.

2. Annealed triblock copolymers

As the sample thermal history is known to play an important role on the copolymers dielectric spectrum [7] the same experiments are performed on samples annealed at 413 K as described in the experimental section. This temperature is chosen as an adequate one to improve the segregation process as compared to samples in the original state, without causing any degradation of the sample. The micrographs

shown in Figs. 2(a–c) are taken after a similar treatment. As the annealing temperature is much higher than the crystallization temperature, i.e., the samples are in the molten state, the changes observed in the crystallinity degree after annealing can only be attributed to contributions from chains that were forming the more diffuse interfaces that sharpens with the thermal treatment. In Figs. 3(a–c) it is clearly shown that steep changes in the relative amount of crystalline matter occur as a result of the annealing for the three triblock copolymers studied here and that trace is represented with a thick line. The annealing increases steeply the amount of crystalline matter in the $S_{57}B_{27}C_{16}$ sample that was almost entirely amorphous in the original state, X_c increasing from 4% to 18%. The same effect is observed in the $S_{35}B_{15}C_{50}$ copolymer where the sample in original conditions showed some crystallinity, $X_c = 23\%$, which is significantly increased after the thermal treatment to 54%, and very sharp reflections appear indicating a growth in the lamellar thickness. For the copolymer with the most abundant PCL component, $S_{09}B_{14}C_{77}$, the effect of the microphase segregation is opposite, as seen in Fig. 3(c) where the crystalline reflections due to PCL have drastically decreased in intensity indicating a decrease in X_c from 53% to 23%. These very significant changes in the degree of crystallinity of the samples, reported in Table III, as a result of a better microphase separation, is also reflected in very important changes in the TSDC spectrum as can be seen in the sequence drawn in Figs. 8(a–c) where the experiments have been performed after polarizing at a temperature near $T_{m\alpha}$ in order to minimize the effect of the intense α' peak located at higher temperatures.

The annealing in $S_{57}B_{27}C_{16}$ and $S_{09}B_{14}C_{77}$, decreases the overall intensity of the TSDC spectrum and has the opposite effect on the $S_{35}B_{15}C_{50}$, which is the only triblock copolymer with an interface PCL-PS as seen in the scheme in Fig. 2(b). These intensity variations are plotted in Fig. 7 (empty symbols) in order to be able to compare the original and annealed samples. In the other two copolymers the PB block forms an intermediate phase between the PCL and the PS segregated structures. The distribution of relaxation time has been calculated with the DSA procedure on the low temperature spectrum and no significant changes are observed either on the position or the profiles of the γ - β region of the TSDC spectrum and the results are reported in Table IV.

The annealing affects only the intensity of the low temperature spectra showing that the amorphous phase that is reorienting is varying in its relative abundance but not in either the Arrhenius relaxation times or their distribution. This variation in the intensity of local modes as well as a similarity in the relaxation parameters have also been observed in semi-interpenetrating polymer networks [32]. The interesting interpretation is how these intensity variations can be related to the variations in crystallinity, to the presence of better defined interfaces between the segregated mesophases and to the existence of a confinement effect. For the original sample $S_{57}B_{27}C_{16}$, the spectrum shown in Fig. 8(a)(filled symbols) the α mode for the PB chains is very visible and approximately as intense as the α mode of PCL. The TSDC spectrum obtained with the annealed sample (empty sym-

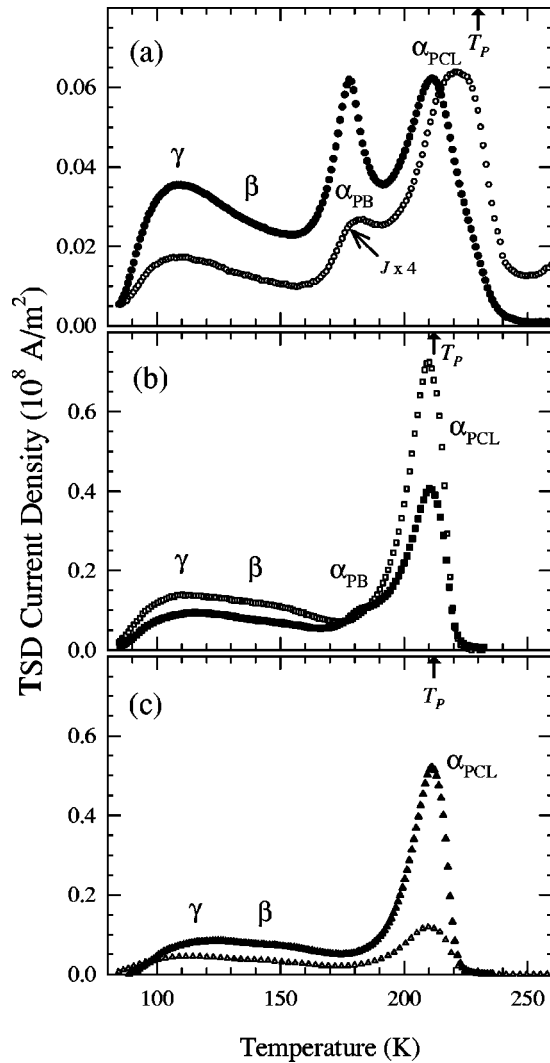


FIG. 8. TSDC spectra ($T < 260$ K) for the original (filled symbols) and annealed (empty symbols) block copolymers. (a) $S_{57}B_{27}C_{16}$, (b) $S_{35}B_{15}C_{50}$, (c) $S_{09}B_{14}C_{77}$. The polarization temperature is indicated by arrows.

is much weaker (the trace in the figure has been multiplied by 4 to make it of comparable intensity with the untreated sample) and shows a shift of the α_{PCL} mode to higher temperatures (221 K). As the effect of the glassy PS chains is screened by the rubbery PB tubes which core is occupied by the PCL chains, which undergo a steep increase in their degree of crystallinity; the stiffening of PCL is to be attributed to the confinement and crystallization effects within the originally cylindrical cores that are deformed to accommodate the PCL crystallites, mainly located at the surface of the flattened PCL cylinders ($L_1 = 30 \pm 6$ nm, $L_2 = 13 \pm 4$ nm) [22]. This crystallization at the interface in block copolymers has been observed in other systems, i.e., poly(tetrahydrofuran)-*b*-poly(isoprene) [33] where the crystalline zones grow at the interface of the lamellar copolymer structure. The drop in the number of mobile entities responsible for the decrease in the intensity of the TSDC spectrum cannot be quantitatively justified by the increase in crystallinity. The additional confinement of the amorphous chains

provided by the crystals existing now in the nanotubes can explain the intensity loss as is the well-documented case in nanopore glasses where intensity of the dielectric trace decreases drastically as the sample is confined in pores of decreasing size [34,35]. The α mode of PB also shows a decrease in its intensity as the result of this enhanced crystallization at the flattened cylinders interface. Nojima *et al.* [36] have studied the crystallization of PCL blocks in diblocks PCL-*b*-PB and they have shown that the effect of the crystallization of the PCL block is strong enough to destroy the micellar structure. In our case the PB block located between the glassy PS chains and the better crystallized PCL after annealing presents a lower mobility as compared to the original state where the PCL block is almost entirely amorphous.

For the triblock copolymer $S_{35}B_{15}C_{50}$ the results are quite different as shown in Fig. 8(b) where the annealed sample is about twice more intense, both in the γ - β and α regions than the sample in the original state. The position of the α peak remains unchanged as well as the distribution of relaxation time extracted with the SADSA numerical procedure. Also, as seen in Fig. 3(b), the WAXS determined crystallinity increases with the thermal treatment (from 23% to 54%) that seems contradictory with the increase in the mobile amorphous phase detected by TSDC. It is to be noted that the lamellar morphology of this triblock copolymer is the only one where there is an interface PS-PCL. The existence of a diffuse interface in the untreated sample is assumed; in this interfacial region PS is blended with the PCL chains that will be restricted in their mobility by the more rigid PS chains in the glassy state. These restrictions hinders the crystallization of PCL as the glass transition of PS is still 70 K above the crystallization temperature of the PCL crystallizable block. Moreover, as the mobile amorphous phase that is dielectrically active shows the same relaxation characteristic parameters as the homopolymer this is indicative that these reorienting PCL chains are unaffected by the PS. When the microphases are best segregated the total amount of amorphous phase decreases but the mobile one increases as shown by the increase in the intensity of the TSDC trace, i.e., the chains originally blended enrich the mobile amorphous phase as well as the crystalline regions. In Fig. 7 the point corresponding to the annealed sample (empty square) falls on the line defined by the homopolymers thus showing that in the annealed state the mobile amorphous phase is very close to the amorphous phase detected in the homopolymers both in the kinetic parameters and in its amount. Several points should be clarified to justify the presence of the blending of PCL with PS in the diffuse lamellar interfaces. First, the presence of a glass transition at temperatures intermediate between that of PCL and PS should be observed as the amount of this missing amorphous phase, dielectrically inactive because of the constraints imposed by the PS chains, is important as seen in Fig. 7 where the point corresponding to the original sample (filled square) falls far below the trend defined by the homopolymers. If the high temperature zone of the TSDC spectra is studied, it is observed that the intensity of the α' relaxation that is attributed to the MWS interfacial polarization, is highest for the $S_{35}B_{15}C_{50}$ triblock copolymer and it is shifted to higher temperatures. Also, it is to

be noted that the TSDC experiments were never carried on at $T > 320$ K in order to avoid the melting of the crystals and a subsequent variation of the amount of amorphous material in the sample. It might be possible that the segmental motion of this mixed phase is hidden under the very intense α' peak (20 times more intense than the α peak) or that it is located at still higher temperatures than the temperature range explored here. Additionally, a mention should be made of the increase in the intensity of the low temperature local relaxations with the annealing that is similar to that of the segmental peak. This evidences a strong hindering effect on the local motions by the presence of miscibility at the interfaces. This is not usually reported in the numerous studies on miscible blends where the miscible blend behaves as a biphasic system at the level of the localized motions that originate the low temperature peaks. For example in the case of miscible PCL/PH (polyphenoxy) studied by dynamic mechanical analysis at 50 Hz there is an effect reported on the local motions of PH chains by the blending with PCL [37].

Finally, the WAXS experiments on the PCL richest triblock copolymer, $S_{09}B_{14}C_{77}$, after the thermal treatment, show an important decrease in the crystallinity degree as shown in Fig. 3(c) (from 53% to 23%), accompanied by a very low intensity of the entire TSDC spectrum recorded after annealing, see Fig. 8(c). The dielectrically active PCL phase has the same relaxation parameters and relaxation time distribution as that of the unrestricted phase in the homopolymer as can be seen in Table IV. The annealed sample has then an important amorphous phase that due to the constraints is not visible by TSDC. This restrained amorphous phase exists in the original sample but its amount is increased by the annealing as it is observed in Fig. 7 by the shift of the point corresponding to the best segregated sample that is farther from the continuous ideal line. The mesophase morphology of this triblock copolymer as shown on the inset of Fig. 2(c) is a PCL matrix with core-shell cylinders where PS is the core and PB is the shell. The peculiarity of the morphology in the well-segregated state is the ellipsoidal cross section of the core-shell cylindrical structure that is attributed to the effect of the crystalline PCL that is apparently forming undulated lamellae, while the amorphous PCL may be occupying the restricted zones between the two-phase cylinders and the crystalline zones [31]. This morphology is the key to understanding the decrease of the unconstrained amorphous phase as shown by the intensity loss in the entire TSDC spectrum that occurs simultaneously with a drop in the crystallinity of the sample. As there is no PS-PCL interface in this mesophases structure, a blending with PS chains cannot be used to explain the constraints that hinders the motions of an important part of the PCL amorphous phase. The relaxation of this rigid amorphous phase is not observed by a higher T_g in the TSDC spectrum whether it is overlapped by the α' peak, which is 20 times more intense than the α peak, or it occurs outside the temperature range explored here. The existence of a rigid amorphous phase that is not undergoing the transition from the glassy to the rubbery state has been demonstrated in several semicrystalline homopolymers such as poly (carbonate of bisphenol A) [38] and poly (ethyleneterephthalate) [39] by dielectric techniques.

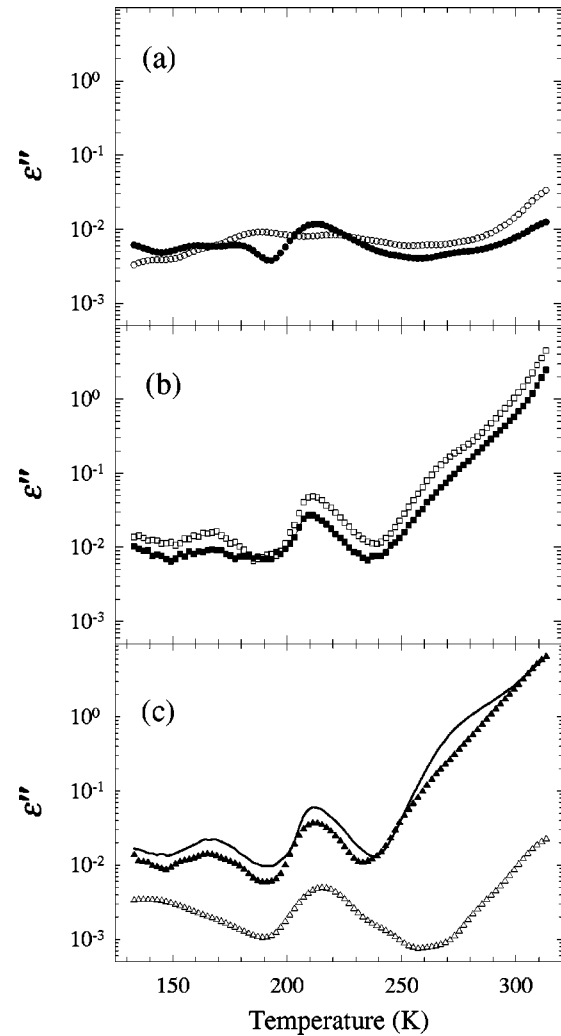


FIG. 9. Dielectric absorption spectra for original (filled symbols) and annealed (empty symbols) block copolymers. (a) $S_{57}B_{27}C_{16}$, (b) $S_{35}B_{15}C_{50}$, (c) $S_{09}B_{14}C_{77}$. The continuous line represents the homopolymer PCL⁹³.

The rigid amorphous regions that are here a very important fraction of the total amount of the amorphous phase in the annealed sample must be a consequence of the constraints imposed by the crystal lamellae and the morphology on the interface. If these restrictions are sufficient to deform the hard-core cylinders, it is reasonable to expect that these constraints are also responsible for the immobilization of an important proportion of the amorphous chains.

D. Broadband dielectric spectroscopy results

The BBDS results agree well with the TSDC ones presented and discussed above for the homopolymer and the three block copolymers. In Figs. 9(a-c) the variation of the imaginary part of the dielectric constant vs temperature $\varepsilon''(T)$ for a frequency of 0.1 Hz for the original samples is presented. The difference in TSDC and BBDS is that the partial depolarization and cleaning procedures that can be achieved in a TSDC experiment are not possible in the dielectric absorption trace that is a dynamic one. Also the influence of the α' peak cannot be minimized by polarizing an

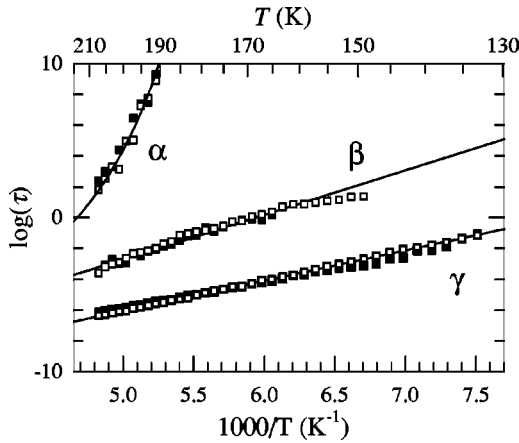


FIG. 10. Relaxation plot, $\log_{10}(\tau) = f(10^3/T)$, for the triblock copolymer $S_{35}B_{15}C_{50}$: (filled squares) original material, (empty squares) annealed sample. The lines are the fitting of the experimental points to VTF (α relaxation) or Arrhenius relaxation times (γ and β modes).

temperatures high enough to activate the α mode but sufficiently low to be unable to induce the trapping process responsible for the high temperature mode. The results are a confirmation of the TSDC results discussed above if we compare the $\epsilon''(T)$ trace to the TSDC one in Fig. 4. The drop in intensity as the wt % in PCL decreases is the same in both cases. The position of the low temperature peaks is shifted in the case of the dielectric absorption results as the variation of the frequency shifts the peaks to higher temperatures as the frequency increases. This effect is larger in the case of the Arrhenius β relaxation than in the case of the VTF relaxation time α mode due to steeper variation of the latter relaxation time as a function of $1/T$. The intensity variations observed after the thermal treatment confirm the results obtained by TSDC techniques, and the discussion on the loss of dielectrically active amorphous mass is applicable here. These variations can be understood by the existence of morphologies that in the annealed state are best segregated and impose together with the crystalline phase whose amount increases for the annealed $S_{35}B_{15}C_{50}$ and $S_{57}B_{27}C_{16}$ constrains that are sufficient to immobilize an important proportion of the amorphous PCL phase. In order to determine the relaxation time distribution in frequency domain the broad peaks are decomposed in Cole-Cole relaxations which is the distribution that best fits the experimental trace for this semicrystalline block. The difficulty resides in the overlap of the various modes in addition to the steep growth recorded at low frequencies due to the conductivity of the sample. Only the fits of the $S_{09}B_{14}C_{77}$ in the original state and the $S_{35}B_{15}C_{50}$ in the original and annealed state are considered satisfactory as they are the most intense and gave reliable results. For example, the VTF energies and preexponential factors are 0.14 eV, 2×10^{-12} s, 0.14 eV, 1×10^{-11} s, 0.12 eV, 1×10^{-12} s, with T_0 values of 156, 162, and 160 K, respectively. The relaxation plots obtained for the $S_{35}B_{15}C_{50}$ in the original and the annealed states are shown in Fig. 10 as $\tau(1/T)$ for the $\alpha, \beta,$

and γ processes. The differences observed for the three samples that were analyzed in detail are not significant due to the difficulty of separating the overlapping peaks. The analysis is done for $T < 210$ K where the merging effects among the α and β processes are not yet observed. The merging of the two processes has been carefully studied in the PCL homopolymer [18] and it has been shown that this merging precedes in temperature a second merging of the α - β mode with the remaining γ mode, with the subsistence at high temperatures and frequencies of one process only. These results compare well with those obtained after the TSDC experiments. The agreement is also found in the relaxation parameters of the β and γ modes where the fit is less precise due to the weak amplitude and strong overlap of these peaks in frequency domain.

E. Conclusions

The triblock SBC copolymers with one semicrystalline block have been characterized by a whole variety of experimental techniques such as DSC, TEM, WAXS, TSDC, BBDS so as to relate the observed dielectric behavior with the crystallinity of the PCL block and the morphology of the segregated mesophases. We have found that the dynamics of the different molecular reorientations occurring in the amorphous phase are similar in the homopolymer and the three copolymers as determined by TSDC and confirmed by dynamic dielectric spectroscopy with a reduction in mobility in the cooperative rearrangements observed only in the case of the annealed triblock copolymer $S_{57}B_{27}C_{16}$. In this case the PCL is confined in nanotubes and the annealing by inducing a higher crystallinity in the block increases the confinement effect on the amorphous regions that provokes a steep intensity decrease in the dielectric response and a shift to higher temperatures. The better microphase segregation obtained after the annealing also results in a growing crystallinity degree of the $S_{35}B_{15}C_{50}$ triblock copolymer with a simultaneous increase of the mobile amorphous phase that is explained by the disappearance of PS-PCL diffuse interfaces present in the original state. The presence of a rigid amorphous phase in $S_{9}B_{14}C_{77}$ constrained by core-shell cylinders with rigid PS core with ellipsoidal cross sections and by undulated lamellae formed by the PCL crystallizing chains, explains the reduction in the TSDC signal after annealing. The dielectric behavior of these complex materials and its variation with a better mesophase segregation show that the constrains imposed by the material morphology and the presence of crystalline lamellae in these restricted geometries affect the local as well as the segmental dynamics in the material.

ACKNOWLEDGMENTS

Financial support from the Consejo Nacional de Investigaciones Científicas y Tecnológicas (CONICIT No. G97-000594) and from the Decanato de Investigaciones y Desarrollo, Universidad Simón Bolívar (Nos. DID-G15 and G02) are gratefully acknowledged.

- [1] K. Karatasos, S.H. Anastasiadis, G. Floudas, G. Fytas, S. Pispas, N. Hadjichristidis, and T. Pakula, *Macromolecules* **29**, 1326 (1996).
- [2] J. Kanetakis, G. Fytas, F. Kremer, and T. Pakula, *Macromolecules* **25**, 3484 (1992).
- [3] K. Adachi, I. Nishi, H. Doi, and T. Kotaka, *Macromolecules* **24**, 5843 (1991).
- [4] J.H. Rosedale and F.S. Bates, *Macromolecules* **23**, 2329 (1990).
- [5] B. Stuhn and F. Stickel, *Macromolecules* **25**, 5306 (1992).
- [6] I. Alig, G. Floudas, A. Avgeropoulos, and N. Hadjichristidis, *Macromolecules* **30**, 5004 (1997).
- [7] K. Karatasos, S.H. Anastasiadis, T. Pakula, and H. Watanabe, *Macromolecules* **33**, 523 (2000).
- [8] A.M. North, R.A. Pethrick, and A.D. Wilson, *Polymer* **19**, 913 (1978).
- [9] A. Kyritsis, P. Pissis, S.M. Mai, and C. Booth, *Macromolecules* **33**, 4581 (2000).
- [10] S. Nojima, K. Hashizume, A. Rohadi, and S. Sasaki, *Polymer* **38**, 2711 (1997).
- [11] J. Heuschen, R. Jerome, and Ph. Teyssié, *J. Polym. Sci., Part B: Polym. Phys.* **27**, 523 (1989).
- [12] S. Nojima, H. Tanaka, A. Rohadi, and S. Sasaki, *Polymer* **39**, 1727 (1998).
- [13] V. Balsamo, F. Von Gyldenfeldt, and R. Stadler, *Macromol. Chem. Phys.* **197**, 1159 (1996).
- [14] V. Balsamo, F. von Glydenfeldt, and R. Stadler, *Macromol. Chem. Phys.* **197**, 3317 (1996).
- [15] O. Urakawa, K. Adachi, T. Kotaka, Y. Takemoto, and H. Yasuda, *Macromolecules* **27**, 7410 (1994).
- [16] A.A. Jones, W.H. Stockmayer, and R.J. Molinari, *J. Polym. Sci., Polym. Symp.* **54**, 227 (1976).
- [17] B. Baysal and W.H. Stockmayer, *Macromolecules* **27**, 7429 (1994).
- [18] M. Grimaud, E. Laredo, M.C. Perez, and A. Bello, *J. Phys. Chem.* **114**, 6417 (2001).
- [19] M.C. Hernandez, E. Laredo, M. Grimaud, and A. Bello, *Polymer* **41**, 7223 (2000).
- [20] J. Vanderschueren, M. Ladang, and J.M. Heuschen, *Macromolecules* **13**, 973 (1980).
- [21] V. Balsamo and R. Stadler, *Macromolecules* **32**, 3994 (1999).
- [22] V. Balsamo, F. von Gyldenfeldt, and R. Stadler, *Macromolecules* **32**, 1226 (1999).
- [23] V. Balsamo and I. Hamley (unpublished).
- [24] I. W. Hamley, *The Physics of Block Copolymers* (Oxford University Press, Oxford, 1998).
- [25] M.L. Arnal, M.E. Matos, R.A. Morales, O.O. Santana, and A.J. Müller, *Macromol. Chem. Phys.* **199**, 2275 (1998).
- [26] V. Balsamo, A.J. Müller, F. von Glydenfeldt, and R. Stadler, *Macromol. Chem. Phys.* **199**, 1063 (1998).
- [27] M. Aldana, E. Laredo, A. Bello, and N. Suarez, *J. Polym. Sci., Part B: Polym. Phys.* **32**, 2197 (1994).
- [28] A. Bello, E. Laredo, and M. Grimaud, *Phys. Rev. B* **60**, 12764 (1999).
- [29] H. Bittiger, R.H. Marchessault, and W.D. Niegisch, *Acta Crystallogr., Sect. B: Struct. Crystallogr. Cryst. Chem.* **B26**, 1923 (1970).
- [30] H. Hu and D. Dorset, *Macromolecules* **23**, 4604 (1990).
- [31] V. Balsamo and R. Stadler, *Macromol. Symp.* **117**, 153 (1997).
- [32] G. Georgoussis, A. Kyritsis, V.A. Bershtein, A.M. Fainleib, and P. Pissis, *J. Polym. Sci., Part B: Polym. Phys.* **38**, 3070 (2000).
- [33] S. Ishikawa and T. Fukutomi, *Eur. Polym. J.* **29**, 877 (1993).
- [34] G. Barut, P. Pissis, R. Pelster, and G. Nimtz, *Phys. Rev. Lett.* **80**, 3543 (1998).
- [35] A. Schönhals and R. Stauga, *J. Chem. Phys.* **108**, 5130 (1998).
- [36] S. Nojima, K. Kato, S. Yamamoto, and T. Ashida, *Macromolecules* **25**, 2237 (1992).
- [37] R. de Juana, R. Hernández, J.J. Peña, A. Santamaría, and M. Cortázar, *Macromolecules* **27**, 6980 (1994).
- [38] E. Laredo, M. Grimaud, A. Müller, A. Bello, and N. Suarez, *J. Polym. Sci., Part B: Polym. Phys.* **34**, 2863 (1996).
- [39] J.C. Coburn and R.H. Boyd, *Macromolecules* **19**, 2238 (1986).